Scientific Journal of Impact Factor (SJIF): 4.72

e-ISSN (O): 2348-4470
p-ISSN (P): 2348-6406

International Journal of Advance Engineering and Research Development

Volume 4, Issue 9, September -2017

Photoelectrochemical Cells of CBD-Coated Cu_2S Nanoparticle-Sensitized ZnO Nanorods

Ganga Shekar Pasupula[1], Shoyeb Mohamad F.Shaikh[1], S.U. Ekar[1], P.V.Shinde[1], R. S. Mane[1], B. N. Pawar[2]

[1]*Centre for Nanomaterials & Energy Devices, School of Physical Sciences,SRTM University, 431606 Nanded, India*
[2]*Dr. B. N. Purandare Arts, Smt. S. G. Gupta Commerce and Science College, Lonavla-410403 (India).*

ABSTRACT:

In present study, Cu_2S nanoparticles (NPs) and ZnO nanorods (NRs) were synthesized using chemical methods and applied in photoelectrochemical cells as an electrode material. The X-ray diffraction spectrums were applied for confirming the respective crystal structures which further were supported by energy dispersive X-ray analysis mappings where elemental composition proportions, as expected, are obtained. From Raman spectroscopy patterns revealed chemical bonds for Cu_2S coated ZnO. Surface morphologies were noticed from the field-emission scanning electron microscopy digital images. By UV-Vis spectroscopy analysis, optical band gap of ZnO decreased from 3.205 eV to 2.78 eV for Cu_2S-ZnO. The power conversion efficiency (η) of Cu_2S-ZnO electrode was 0.160% which was 0.07% for ZnO. This increment was assigned to the decrease of the charge transport resistance from 95 to 79Ω in electrochemical impedance spectroscopy measurement.

Keywords: *SILAR, CBD, ZnO Nanorods,Cu_2S NPs, Photoelectrochemical Cells.*

I. INTRODUCTION

Inorganic metal chalcogenide nanoparticles (NPs) sensitised solar cells are attracting the researchers a great attention. Especially, the combination of wide band gap semiconductors ZnO, TiO_2, SnO_2, Bi_2O_3 etc., with a low band gap inorganic metal chalcogenide like CdS, CdSe, CdTe, In_2S_3 etc., is playing a great role in photoelectrochemical solar cells. ZnO, II-VI group, due to its wide band gap energy (3.2 eV) nature, absorbs most of UV light whereas, copper sulphide or copper selenide (Cu_2S or Cu_2Se) due to its low band gap absorb both visible as well as UV light. Wurtzarite hexagonal structure of ZnO has several applications like in gas sensors [1], solar cells [2], photo catalysts [3], and so on. Different kinds of morphologies like nano-beads [4], nano-rods [2, 5], nano-sheets [6], nano-flowers [7] and so on have been synthesized so far by using various chemical and physical synthesis methods like chemical bath deposition (CBD) [1], chemical vapour deposition [5], hydrothermal [8], successive ionic layer adsorption and reaction (SILAR) [9], and so on. The Cu_2S or Cu_2Se is receiving considerable attention among the metal chalcogenides family. The Cu_2S exists in the forms of monoclinic, hexagonal and cubic. The monoclinic structure is available at lower temperatures. Cu_2S thin films have attracted noticeable attention due to their wide range of applications such as gas sensors [10], field emission studies [11], solar cells [12], switching devices [13], opto-electronic devices [14] and so on. Several methods like SILAR [15], CBD [16], spray pyrolysis [17], hydrothermal [18], ultrasonic method [19] and so on have been so far preferred to synthesize them in thin/thick film forms. Various morphologies like nanowires, nano disks, nanorods, nano plates, nano crystals [20-24] are on the credit of Cu_2S. In addition, Cao *et. al* reported ZnO modification using wide and narrow band gap semiconductors such as ZnS, ZnSe, Bi_2S_3, and Cu_2S for photoelectrochemical application [25]. The CBD method is extremely attractive since this method possesses numerous advantages over conventional thin films deposition methods. It can be carried out in glass beakers. The starting materials are commonly available and cheap. The main benefits of this method include low temperature deposition, low synthesis cost and easy coating of large surfaces. With SILAR mediated synthesis of ZnO NPs as seeding layer ZnO NRs were obtained by CBD method and then by CBD-deposition of Cu_2S NPs layer was obtained to form Cu_2S-ZnO whose photoelectrochemical cell performance was investigated.

II. EXPERIMENTAL DETAILS

2.1. Deposition of CBD-mediated Cu_2S NPs on SILAR-based ZnO NRs

All the chemicals were of analytical grade and used for the experiment without purification. To prepare zinc nitrate hexahydrate ($Zn(NO_3)_2.6H_2O$), 1.49 gm ($Zn(NO_3)_2.6H_2O$) was taken into a beaker of 50 ml capacity. Double distilled water was used to prepare 0.1. M final stock solution. Aqueous ammonia (NH_4OH) solution was added in to stock solution so as to increase pH from nearly neutral to 12. On adding excess ammonium solution the milky coloured solution of zinc salt was turned into clear i.e. transparent. As discussed earlier two methods i.e. SILAR and CBD were used for the formation of ZnO on ITO and then for loading Cu_2S on pre-deposited ZnO nanorods (NRs), CBD was preferred as to form Cu_2S-ZnO. For the deposition of ZnO by seeding layer method, Zn precursor solution (Ammonia complexed zinc nitrate hexahydrate) was kept at room temperature (27 ^oC), while

the hot distilled water was maintained at 91 °C. The seeding layer deposition was carried by dipping the transparent indium-tin-oxide (ITO) substrate periodically into these solution beakers. After 5 cycles a whitish film was formed to be observed on the ITO substrate. The CBD double deposition was carried to get the good ZnO NRs onto a seeding layer deposited ZnO-ITO substrate at 91 °C for 1 h in each deposition. Then after the ZnO film composed of NRs was washed with distilled water and used for depositing another sensitizing NPs i.e. Cu_2S.

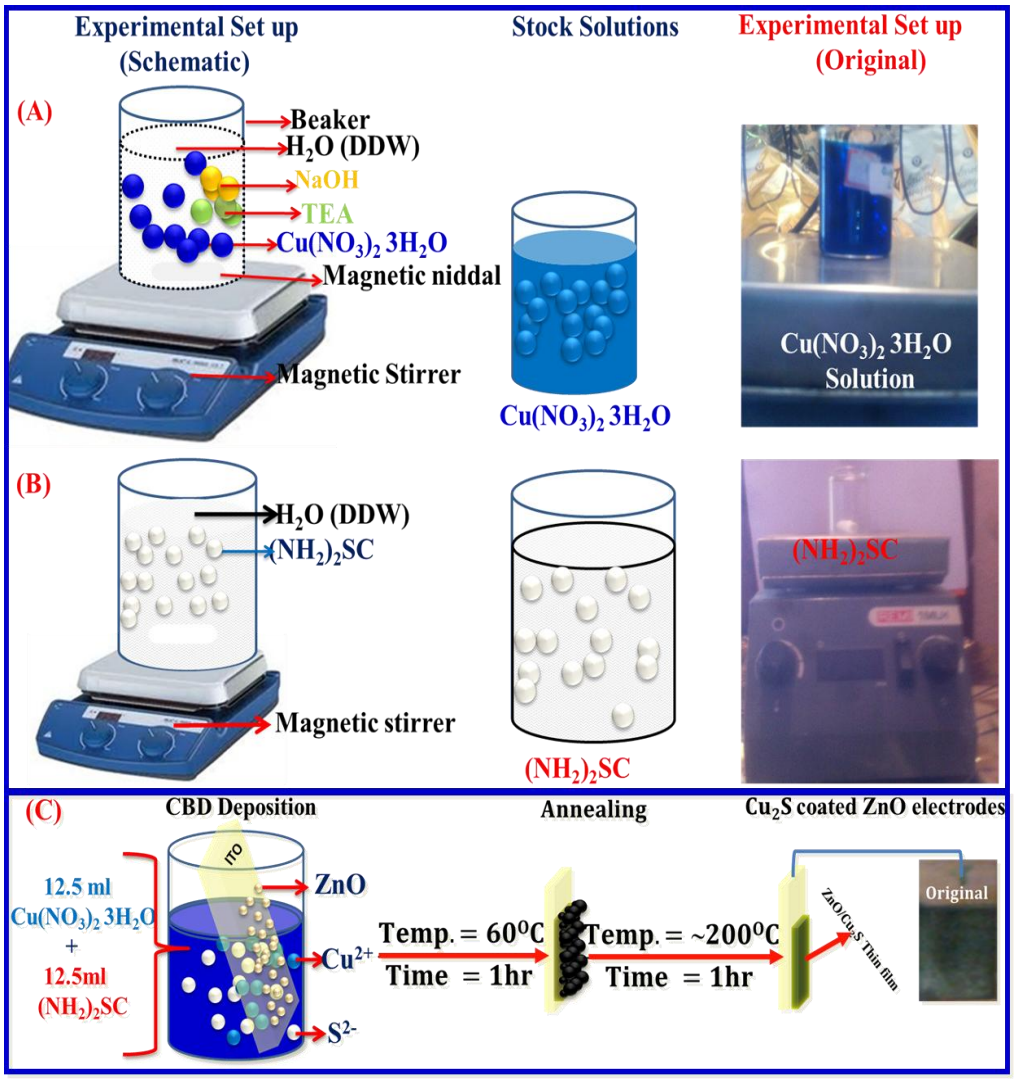

Fig. 1: (A) Preparation of $Cu(NO_3)_2.3H_2O$ solution, (B) Preparation of $(NH_2)_2SC$ solution,(C) Approach of Cu_2S-ZnO formation.

The Cu_2S NPs film was deposited onto ZnO NRs. For this purpose, $Cu(NO_3)_2.3H_2O$, and $(NH_2)_2SC$ chemicals were chosen as the sources for Cu and S elements. In the first phase, $Cu(NO_3)_2.3H_2O$,and $(NH_2)_2SC$ solutions were prepared in 0.05:0.1 M molar ratio (volumetric ratio of 1:2 ml and mass ratio of 1.21:0.7612). Now, $Cu(NO_3)_2.3H_2O$ solution was prepared in a 50 ml capacity beaker using $Cu(NO_3)_2.3H_2O$ followed by an addition of H_2O and appropriate amount of tri-ethanol-amine (TEA) and the beaker with solution was placed for stirring. To maintain the pH, few sodium hydroxide pellets were added slowly [Fig. 1(A)]. After this, $(NH_2)_2SC$ solution was prepared by using $(NH_2)_2SC$ and DDW in a 100 ml capacity beaker, which was well clear and transparent [Fig.1 (B)]. In the second phase, $Cu(NO_3)_2.3H_2O$ and $(NH_2)_2SC$ solutions were taken in a separate 25 ml beaker to prepare Cu-S mixed solution. For this purpose, 12.5 ml volume of each i.e. $Cu(NO_3)_2.3H_2O$ and $(NH_2)_2SC$ were mixed to prepare 25 ml Cu-S stock solution. In third phase, previously coated ZnO NRs films were immersed into this solution beaker vertically inclined to the wall of the beaker in such a way that ZnO thin film surface was towards the mixed solution side and non-conducting surface towards the wall of the beaker side for 1 h at pH~9 at the constant bath temperature of 60 ^oC. After the deposition, the film i.e. Cu_2S-ZnO was taken out and rinsed with DDW and dried in air. For removing hydroxides or salts if there is any, the as-deposited films were air-annealed at ~200 ^oC for 1 h. After this Cu_2S-ZnO was taken and the film obtained at non-conducting side was erased neatly and used in the rest of the measurements. The growth process of Cu_2S-ZnO electrode has been given in Fig. 1(C).

III. RESULTS AND DISCUSSION

3.1. Surface morphology and structural studies

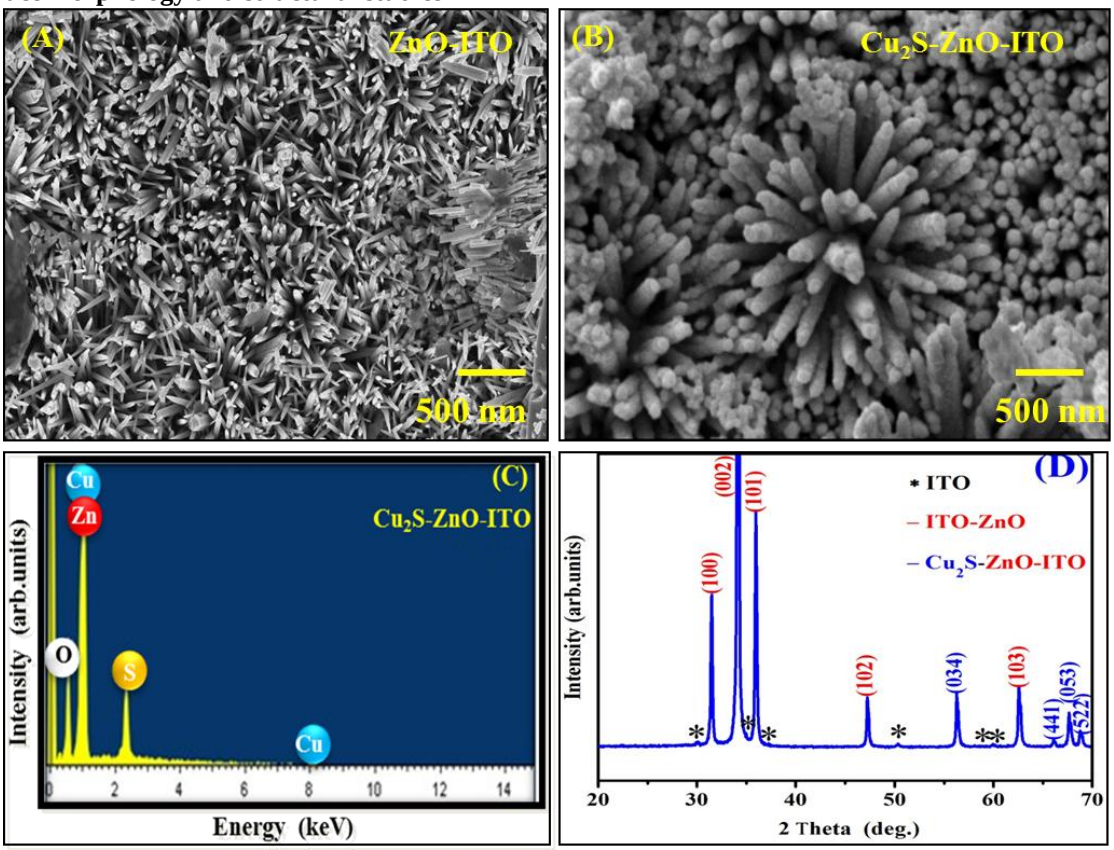

Fig. 2: (A) and (B) FE-SEM images of ZnO, and Cu_2S-ZnO, (C) EDAX images of Cu_2S sensitised ZnO electrodes, and (D) XRD images of Cu_2S sensitised ZnO electrodes

FE-SEM images were used to study the surface morphology of ZnO and Cu_2S-ZnO electrodes. Fig. 2(A) shows the FE-SEM image of ZnO where the surface appearance of hexagonal structure and NR-type morphology are noticed. These NRs are nearly 500 nm in sizes.

These ZnO NRs are arbitrarily organized with various diameters (~150 nm) and lengths (300 nm). Their heights are unprecedented as they are well inserted in. Believe that this type of morphology can offer high surface area, high aspect ratio and also good continuity for charge transportation due to their long lengths. When the Cu_2S NPs were deposited on ZnO, then the surface vision is changed from polished to [Fig. 2(B)] rougher one. It means Cu_2S was in the form of NPs which, upon deposition, have covered complete surface of the ZnO NRs with diameters in the range of ~ 200 nm and lengths ~500 nm.

To identify the presence of the elements in Cu_2S-ZnO, the elemental compositional study was performed by using EDAX spectroscopy coupled with FE-SEM unit. The EDAX spectrum reveals Zn, O, Cu and S elements over the surface of Cu_2S-ZnO, providing quantitative evidence for existence of Cu-S and Zn-O in Cu_2S-ZnO (Fig. 2(C)).

The structural properties of Cu_2S-ZnO films were studied using XRD pattern recorded by using an X-ray diffractometer with $CuK\alpha_1$ radiations (λ=1.5406 Å) in 2θ range from 20°-70° and is given in Fig. 2(D).Peaks marked by an asterisk (∗) are of ITO i.e. substrate used. The XRD peaks at 31.39°,34.15°,36.50°,47.58° and at 62.83° respectively are due to (100),(002),(101),(102) and (103) reflection planes of wurtzite (hexagonal) ZnO [JCPDS No: 36-1451]. Additional peaks in XRD spectrum at 2θ = 56.25°, 66.14°, 67.60 and at 68.93° are indexed to the (034), (441), (053), and (522) crystal planes of Cu_2S, respectively [JCPDS NO: 33-0490]. Obtained peaks have supported for the formation of the monoclinic crystal structure of Cu_2S on wurtzite ZnO so as to form Cu_2S-ZnO.

3.2 Optical study

The prevailing technique for examining the vibrational properties of the deposited films is the Raman spectroscopy. The Raman spectrum of Cu_2S-ZnO was scanned in the spectral range of 0-800 cm^{-1} by using Raman scattering system with an Olympus microscope. Fig.3 shows the Raman spectroscopy measurement peaks of Cu_2S-ZnO. The Raman peaks observed at around 103 cm^{-1} and 438 cm^{-1} are attributed to E_2 (low) and E_2 (high) phonon modes of

ZnO and peaks located at 331 cm^{-1} and 574 cm^{-1} are attributed to $A_{1\ (TO)}$ and $E_{1(LO)}$ Raman bands. Peaks at around 290 cm^{-1} and 473 cm^{-1} are due to Cu_2S, suggesting the presence of Cu_2S on ZnO.

Absorption spectra of ZnO and Cu_2S-ZnO were obtained on UV-vis spectrophotometer (WantechWPG-100 Potentiostat/Galvanostatic) in the wavelength range between 350 -700 nm. The absorption data were analysed to estimate the respective energy band gap by using the Tuac's relationship given in equation (1) [26].

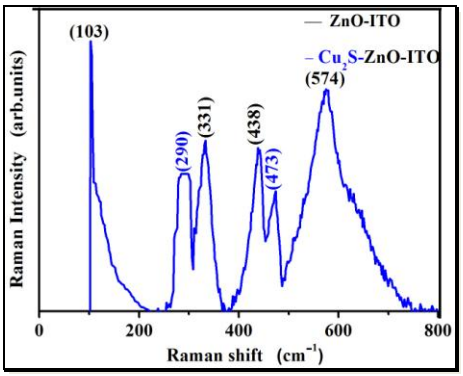

Fig. 3: Raman images of Cu_2S sensitised ZnO electrodes

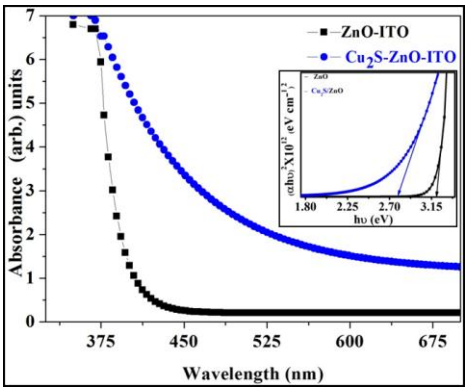

Fig 4: UV-VIS spectra of ZnO and Cu_2S-ZnO (inset: estimation of respective band gap energies).

Fig. 4 shows the absorbance peaks of ZnO and Cu_2S-ZnO electrodes. As-prepared ZnO NRs film [Fig. 4] confirms a little absorbance in the UV region (< 400 nm wavelength) whereas, Cu_2S-ZnO electrode has demonstrated enhanced absorbance in the visible region (≥ 400 nm wavelength). Thus, Cu_2S-ZnO film electrode composed of both NPs and NRs morphologies reveals an enhanced absorbance in visible region.

The relationship between the absorption coefficient "α" and the photon energy "hν" is given by Tauc's relation as;

$$\alpha = \frac{\alpha_o (h\nu - E_g)^n}{h\nu} \qquad (1)$$

where E_g = optical band gap, h = plank's constant, n = constant. The inset of Fig. 4 represents the Tuac's plots for ZnO and Cu_2S-ZnO electrodes which were to estimate the energy band gaps. The plot of "$\alpha h\nu^2$" against "hν" is linear and X-intercepts of the plot $\alpha h\nu^2$ against $h\nu$ offered energy band gaps for ZnO and Cu_2S-ZnO electrodes which are respectively 3.205 and 2.78 eV.

3.3. Photo-electrochemical cell and electrochemical impedance spectroscopy measurements

The current density–applied voltage (J–V) measurements of ZnO and Cu_2S-ZnO electrodes were performed using IGOR program and Keithley-2400 power sources meter (Solar Simulator) *under 1 Sun light intensity and 0.28 cm^2 exposed surface area* and are shown in [Fig.5].

3.3.1. Fabrication of solar cells

The Cu_2S-ZnO electrode solar cell was assembled with a platinum coated FTO as counter electrode and Cu_2S-ZnO as working electrode. The polysulphide electrolyte solution was injected between the electrodes spacing to complete the cell assembly. The preparation of polysulphide electrolyte solution was followed by taking equal molars of Na_2S, NaOH and S (0.1M each).

The solar cell performance characteristics like open circuit voltage, short circuit current density, fill factor and power conversion efficiency etc., are designated as V_{oc}, I_{SC}, FF and η%, respectively. These parameters were calculated were obtained from J-V plots and are tabulated in Table 1. The solar cell efficiency for Cu_2S sensitised ZnO electrodes (0.16%) was observed to be greater than ZnO (0.07%).This is due to the fact that when Cu_2S NPs were sensitised on ZnO-ITO, then band gap of Cu_2S-ZnO electrode was narrowed. This narrow band gap provides more number of photons absorption and resulting in the generation of number charge carriers. This leads to the enhanced current density and hence efficiency. Thus, from the J-V analysis of ZnO and Cu_2S-ZnO electrodes, it was concluded that composite solar cell consisting of wide band gap ZnO-narrow band gap Cu_2S yielded enhanced photoconversion conversion efficiency than ZnO.

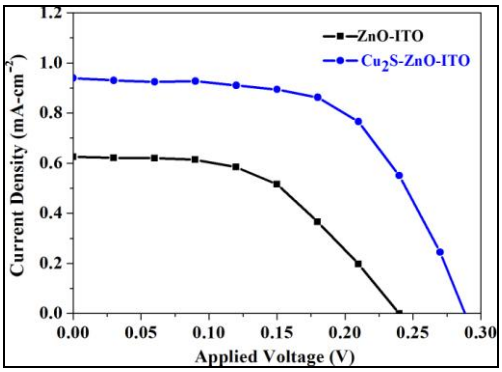

Fig. 5: JV plots of ZnO and Cu_2S-ZnO electrodes.

Table 1: Photoelectrochemical cell parameters of ZnO and Cu_2S-ZnO electrodes

S.NO.	Working electrode	V_{OC} (V)	I_{SC} (mA-cm^{-2})	FF	η%
1	ZnO-ITO	0.24	0.61	0.52	0.07%
2	Cu_2S sensitised ZnO-ITO electrodes	0.29	0.94	0.59	0.16%

The properties of the photoelectrochemical cells like ionic and electronic processes can be obtained by using EIS (Model CHI6112D). EIS is a powerful technique to find the impedance of the materials as the function of varying the frequency of the voltage signal applied to determine the resistance and capacitances of the photo-anode/photocathode materials. The two arcs in the Fig 6, i.e.one in the low frequency and the second in the high frequency regions are obtained. The arc in the low frequency region corresponds to charge transfer at electrolyte-photo anode and the arc in the high frequency region corresponds to the charge transfer at counter electrode-electrolytes, respectively.The charge transport resistance was decreased from 95 to 79 Ω when Cu_2S NPs were deposited on ZnO NRs.

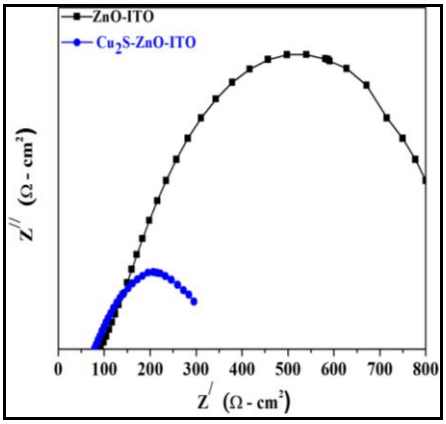

Fig. 6: Nyquist plots of ZnO and Cu_2S-ZnO electrodes

IV. CONCLUSIONS

In summary, the ZnO NRs were synthesised by using SILAR and CBD double deposition methods. For growing ZnO NRs, few cycles of SILAR were applied due to which seeding layer for growing ZnO NRs was developed. The inorganic Cu_2S NPs were deposited on ZnO NRs to form Cu_2S-ZnO electrode on ITO substrates which was used for photoelectrochemical studies. Due to increase in optical absorbance; band gap energy of Cu_2S-ZnO electrode was smaller than ZnO which decreased charge transport resistance followed by increase of power conversion efficiency to 0.16 % from 0.07%.

REFERENCES

[1] C.D. Lokhande, P.M. Gondkar, R. S. Mane, V.R. Shinde, Sung-Hwan Han, CBD grown ZnO-based gas sensors and dye-sensitized solar cells, J. of Alloys and Compounds, 475 (2009) 304–311.
[2] S.B. Ambade, R. B. Ambade, W. Lee , R.S. Mane, S.C.Yoon, S.H. Lee, Development of highly transparent seedless ZnO nanorods engineered for inverted polymer solar cells, Nanoscale,6 (2014) 12130-12141.
[3] J. Liqiang, W. Baiq, X. Baifu, L. Shudan, S. Keying, C. Weimin, F. Honggang, Investigations on the surface modification of ZnO nanoparticle photocatalyst by depositing Pd, J. of Solid State Chem., 177 (2004) 4221–4227.
[4] V.R. Shinde, T.P. Gujar, C.D. Lokhande, Enhanced response of porous ZnO nanobeads towards LPG: Effect of Pd sensitization, Sensors and Actuators B, 123 (2007) 701–706.
[5] D.C. Kim, B.H. Kong, H.K. Cho, D.J. Park, J.Y. Lee, Effects of buffer layer thickness on growth and properties of ZnO nanorods grown by metal organic chemical vapour deposition, Nanotechnology, 18 (2007) 015603.
[6] Sun-Ki Min, Rajaram S. Mane, Oh-Shim Joo, T. Ganesh, Byung Won Cho, Sung-Hwan Han,Upright-standing ZnO nano-sheets growth using wet chemistry, Current Applied Physics, 9 (2009) 492–495.
[7] K.M.Kumar, B.K. Mandal, E.A. Naidu, M. Sinha, K.S. Kumar, P.S. Reddy, Synthesis and characterization of flower shaped zinc oxide nanostructures and its antimicrobial activity, Spectrochimica Acta Part A: Molecular and Biomolecular Spectroscopy, 104, (2013) 171–174.
[8] S. Baruah, J. Dutta, Hydrothermal growth of ZnO nanostructures, Science and Technology of Advanced Materials,10 (2009) 013001.
[9] D. D. Haridas, K.S. Shinde, N. B. Velhal , G.M. Lohar, V. J. Fulari, Synthesis and characterization of ZnO thin film by low cost modified SILAR technique, AIMS Materials Science, 3 (2016) 349-356.
[10] A.A. Sagade, R.Sharma, Copper sulphide (Cu_xS) as an ammonia gas sensor working at room temperature, Sens Actuators B, 133 (2008) 135–143.
[11] X.P. Feng, Y.X. Li, H.B. Liu, Y.L. Li, S. Cui, N. Wang, L. Jiang, X.F. Liu, M.J. Yuan, Controlled growth and field emission properties of CuS nanowalls, Nanotechnology, 18 (2007) 145706.
[12] S. R. Das, V. D. Vankar, P. Nath, and K. L. Chopra, "The preparation of Cu_2S films for solar cells," Thin Solid Films, 51 (1978) 257–264.
[13] T. Sakamoto, H. Sunamura, H. Kawaura, T. Hasegawa, T. Nakayama, M. Aono, Nanometer-scale switches using copper sulfide, Appl Phys Lett., 82 (2003) 3032–3034.
[14] R. Sharma, A. A. Sagade, S.R. Gosavi, Y.Ganesh Gudage, A. Ghosh, P. Kulariya, I. Sulaniya ,R.S. Mane,S.H. Han, Effect of high electronic energy loss of 100 MeV gold heavy ions in copper chalcogenides (CuX, X = S, Se) at nanoscale: Opto-electronic properties study, J. of Non-Crystalline Solids, 355 (2009) 1653–1658.
[15] S. D. Sartale, C.D. Lokhande, Growth of copper sulphide thin films by successive ionic layer adsorption and reaction (SILAR) method, Materials Chemistry and Physics, 65 (2000) 63-67.
[16] S. U. Offiah, P. E. Ugwoke, F. I. Ezema, A. B. C. Ekwealor, R. U. Osuji, Comparative study of Cu_xS and Cu_ySe thin films grown by CBD, Chalcogenide Letters., 2 (2012) 257-264.
[17] W. Y. Kim, B. M. Palve, H. M. Pathan, and O. S. Joo, Spray pyrolytic deposition of polycrystalline Cu_2S thin films, Materials Chemistry and Physics, 131 (2011) 525–528.
[18] X.Yu , X. An, Controllable hydrothermal synthesis of Cu_2S nanowires on the copper substrate, Materials Letters, 64 (2010) 252–254.
[19] M.K. Mehdi, S.N. Masoud, R.Majid, Preparation and characterization of Cu_2S nanoparticles via ultrasonic method, J Clust Sci., 24 (2013) 927–934.
[20] Z.P. Liu, D. Xu, J.B. Liang, J.M. Shen, S.Y. Zhang, Y.T. Qian, Growth of Cu_2S ultrathin nanowires in a binary surfactant solvent, The Journal of Physical Chemistry B, 109 (2005) 10699–10704.
[21] Y.B. Chen, L. Chen, L.M. Wu, The structure-controlling solventless synthesis and optical properties of uniform Cu_2S nanodisk, Chemistry-A European Journal, 14 (2008) 11069–11075.
[22] T.H. Larsen, M. Sigman, A. Ghezelbash, R. Christopher Doty, B.A. Korgel, Solventless synthesis of copper sulfide nanorods by thermolysis of a single source thiolate-derived precursor, J Am Chem Soc., 125 (2003) 5638–5639.
[23] H.T. Zhang, G. Wu, X.H. Chen, Large-scale synthesis and self-assembly of monodisperse hexagon Cu_2S nanoplates, -Langmuir, 21 (2005) 4281–4282.
[24] Y. Wu, C. Wadia, W. Ma, B. Sadtler, A.P. Alivisatos, Synthesis and photovoltaic application of copper (I) sulfide nanocrystals, Nano Lett., 8 (2008) 2551–2555.
[25] Pen Chen, Li Gu and Xuebo Cao, From single ZnO multipods to heterostructured ZnO/ZnS, ZnO/ZnSe, ZnO/Bi_2S_3 and ZnO/Cu_2S multipods: controlled synthesis and tunable optical and photo electrochemical properties, Cryst Eng Comm, 12 (2010) 3950–3958.
[26] J. Tauc, R. Grigorovici, A. Vancu,Optical properties and electronic structure of amorphous germanium, Phys. Status Solidi B, 15 (1996) 627-637.

